Infrared Spectroscopic and Density Functional Theory Studies on the Reactions of Yttrium and Lanthanum Atoms with Nitrous Oxide in Excess Argon

Ling Jiang and Qiang Xu*

National Institute of Advanced Industrial Science and Technology (AIST), Ikeda, Osaka 563-8577, Japan

Received: March 11, 2008; Revised Manuscript Received: May 3, 2008

Reactions of laser-ablated Y and La atoms with N_2O molecules in excess argon have been investigated using matrix-isolation infrared spectroscopy. Metal monoxide−dinitrogen complexes, $OM(N_2)$ (M = Y, La) and OYNN, have been formed during sample deposition and identified on the basis of isotopic shifts, mixed isotopic splitting patterns, and CCl_4-doping experiments. The $OYNN^+$ and $OLaNN^+$ cation complexes appear during sample deposition and increase visibly upon broad-band irradiation ($\lambda > 250$ nm) at the expense of the neutral metal monoxide−dinitrogen complexes. Density functional theory calculations have been performed on the products. The agreement between the experimental and calculated vibrational frequencies, relative absorption intensities, and isotopic shifts supports the identification of these species from the matrix infrared spectra. Furthermore, a plausible reaction mechanism for the formation of these products has been proposed.

Introduction

Nitrous oxide (N_2O) is isoelectronic with carbon dioxide (CO_2) but exhibits a global warming potential about 310 times that of CO_2 on a per molecule basis.[1] N_2O also acts as a potentially clean and highly selective oxygen donor for catalytic oxidation processes.[2] Gas-phase reactions of various metal atoms with N_2O have been extensively investigated both experimentally and theoretically.[3–11] It has been found that the reaction of transition-metal atoms with N_2O leads to N−O bond activation to form the metal oxide and N_2. The reactions were predicted to proceed via the initial formation of a weakly bound complex. Temperature-dependent measurements revealed activation energies between 2 and 80 kcal/mol.[3–11] Excited-state metal atoms were found to react easily.[3–11]

Several reaction mechanisms have been proposed to account for the kinetics of the reactions of N_2O with 3d transition metals.[4–8,10,12] The electron-transfer mechanism[4,5,12] suggests that the key step is an electron transfer from the metal atom to N_2O following the harpoon mechanism.[12] The direct abstraction mechanism[4,5] accounts for the increasing reactivity of the excited metal atoms. The resonance-interaction mechanism[6–8] accurately estimates barriers for reactions with alkali and alkaline earth metals[6] but works less successfully for transition-metal atoms,[11] which can be attributed to the neglect of the d electrons in the model. The mechanism of electron-transfer-assisted oxygen abstraction[10] assumes that the reactions are initiated by an electron transfer from the metal atom to N_2O.

Recent studies have shown that, with an aid of an isotopic substitution technique, matrix-isolation infrared spectroscopy, combined with quantum chemical calculations, is very powerful in investigating the spectrum, structure, and bonding of novel species.[13,14] Recently, argon matrix investigations of the reactions of laser-ablated Sc, Ti, and groups 10 and 13 metal atoms with N_2O have characterized a series of metal monoxide−dinitrogen and metal nitrous oxide complexes.[15–18] Copper and silver chloride−nitrous oxide complexes ClCuNNO and ClAgNNO have also been obtained in the reactions of metal chlorides with nitrous oxide.[19] Here, we report a study of the reactions of laser-ablated yttrium and lanthanum atoms with nitrous oxide in excess argon. We will show that the metal monoxide−dinitrogen complexes, $OM(N_2)$ (M = Y, La) and OYNN, are formed during sample deposition. The $OMNN^+$ cation complexes appear during sample deposition and increase visibly upon broad-band irradiation ($\lambda > 250$ nm) at the expense of the neutral metal monoxide−dinitrogen complexes.

Experimental and Theoretical Methods

The experiments for laser ablation and matrix-isolation infrared spectroscopy are similar to those previously reported.[20] In short, the Nd:YAG laser fundamental (1064 nm, 10 Hz repetition rate with 10 ns pulse width) was focused on the rotating Y (99.9%, Kojundo Chemical Lab Co.) and La (99.9%, Kojundo Chemical Lab Co.) targets. The laser-ablated Y and La atoms were co-deposited with N_2O in excess argon onto a CsI window cooled normally to 4 K by means of a closed-cycle helium refrigerator. Typically, a 1−12 mJ/pulse laser power was used. N_2O (99.5%, Taiyo Nippon Sanso Co.), $^{15}N_2O$ (98%, Cambridge Isotopic Laboratories), and $^{14}N_2O + {}^{15}N_2O$ mixtures were used in different experiments. In general, matrix samples were deposited for 30−60 min with a typical rate of 2−4 mmol per hour. After sample deposition, IR spectra were recorded on a BIO-RAD FTS-6000e spectrometer at 0.5 cm^{-1} resolution using a liquid-nitrogen-cooled HgCdTe (MCT) detector for the spectral range of 5000−400 cm^{-1}. Samples were annealed at different temperatures and subjected to broad-band irradiation ($\lambda > 250$ nm) using a high-pressure mercury arc lamp (Ushio, 100 W).

Density functional theory (DFT) calculations were performed to predict the structures and vibrational frequencies of the observed reaction products using the Gaussian 03 program.[21] All of the present computations employed the BP86 density functional method, but comparisons were done with the B3LYP density functional method as well.[22] The 6-311+G(d) basis set was used for the N and O atoms,[23] and the scalar-relativistic SDD pseudopotential and basis set were used for the Y and La atoms.[24] Geometries were fully optimized, and vibrational

* To whom correspondence should be addressed. E-mail:q.xu@aist.go.jp.

10.1021/jp802114z CCC: $40.75
Published on Web 06/21/2008

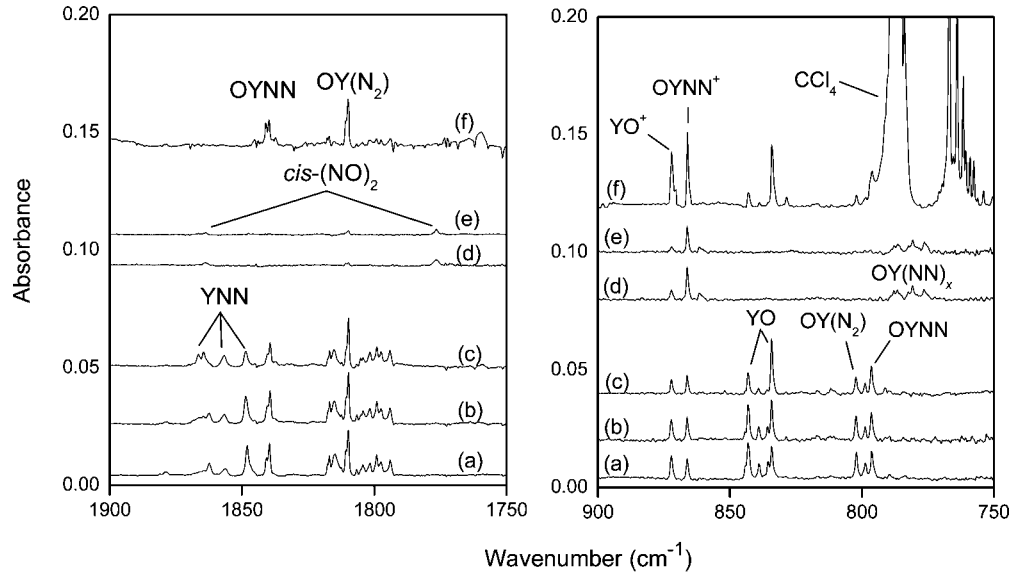

Figure 1. Infrared spectra in the 1900−1750 and 900−750 cm^{-1} regions from co-deposition of laser-ablated Y atoms with 0.2% N_2O in Ar at 4 K. (a) Spectrum obtained from the initial sample deposited for 1 h, (b) spectrum after annealing to 30 K, (c) spectrum after annealing to 34 K, (d) spectrum after 10 min of broad-band irradiation, (e) spectrum after annealing to 38 K, and (f) spectrum obtained by depositing laser-ablated Y atoms with 0.2% N_2O + 0.03% CCl_4 in Ar at 4 K for 1 h and annealing to 34 K.

frequencies were calculated with analytical second derivatives. Transition-state optimizations were done with the QST3 algorithm[25] within the synchronous transit-guided quasi-Newton (STQN)[26] method, followed by the vibrational calculations showing the obtained structures to be true saddle points. The intrinsic reaction coordinate (IRC)[27] method was used to track minimum-energy paths from transition structures to the corresponding local minima. A step size of 0.1 $amu^{1/2}$ bohr was used in the IRC procedure. Recent investigations have shown that such computational methods can provide reliable information for metal complexes, such as infrared frequencies, relative absorption intensities, and isotopic shifts.[15–17,28]

Results and Discussion

Experiments have been done with nitrous oxide concentrations ranging from 0.02 to 1.0% in excess argon. Typical infrared spectra for the reactions of laser-ablated Y and La atoms with N_2O molecules in excess argon in the selected regions are illustrated in Figures 1–4, and the absorption bands in different isotopic experiments are listed in Table 1. The stepwise annealing and irradiation behavior of the product absorptions is also shown in the figures and will be discussed below. Experiments were also done with different concentrations of CCl_4 serving as an electron scavenger.[29]

Quantum chemical calculations have been carried out for the possible isomers and electronic states of the species involved in the M + N_2O reactions. Present calculations show that the BP86 and B3LYP methods give similar geometrical parameters. Hereafter, mainly BP86 results are presented for discussion. The comparison of the observed and calculated IR frequencies and isotopic frequency ratios for the N−O and M−O stretching modes of the products are summarized in Table 2. The ground electronic states, point groups, vibrational frequencies, and intensities of the products are listed in Table 3. Figure 5 shows the optimized structures and the relative energies of the species involved in the M + N_2O reactions. Figure 6 depicts the potential energy surface of the reaction of N_2O with the yttrium and lanthanum atoms. Molecular orbital depictions of the highest occupied molecular orbitals (HOMO) of the

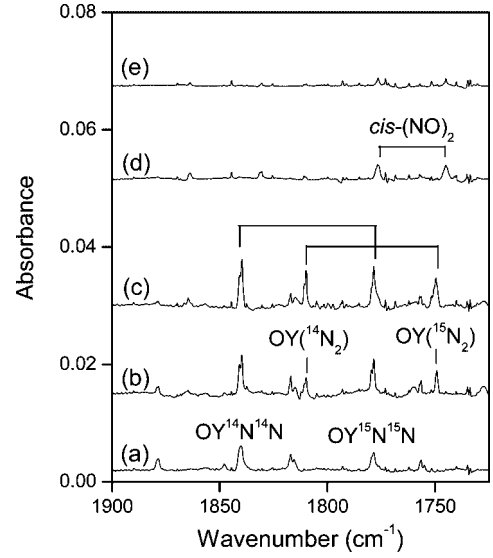

Figure 2. Infrared spectra in the 1890−1740 cm^{-1} region from co-deposition of laser-ablated Y atoms with 0.15% $^{14}N_2O$ + 0.15% $^{15}N_2O$ in Ar at 4 K. For the meaning of (a−e), see Figure 1.

$OM(N_2)$, OYNN, and $OMNN^+$ (M = Y, La) complexes are illustrated in Figure 7.

A. $OM(N_2)$ and OYNN (M = Y, La). In the reaction of Y atoms with N_2O in the argon matrix, absorptions at 1809.8 and 802.3 cm^{-1} that appear together during sample deposition change little after sample annealing but disappear upon broad-band irradiation and do not reappear after further annealing to higher temperature (Table 1 and Figure 1). The upper band at 1809.8 cm^{-1} shifts to 1749.7 cm^{-1} with $^{15}N_2O$, exhibiting an isotopic frequency ratio ($^{14}N_2O/^{15}N_2O$, 1.0343) characteristic of a N−N stretching vibration. The mixed $^{14}N_2O$ + $^{15}N_2O$ isotopic spectra (Figure 2) only provide the sum of pure isotopic bands, which indicates that only one N_2 unit is involved in the complex.[30] The 802.3 cm^{-1} band, which is in the spectral range expected for the terminal Y−O stretching mode,[31] shows no nitrogen isotopic shift. It is noted that the behavior with annealing and irradiation of another group of bands at 1839.4 and 796.5 cm^{-1} is similar to that of the 1809.8 and 802.3 cm^{-1}

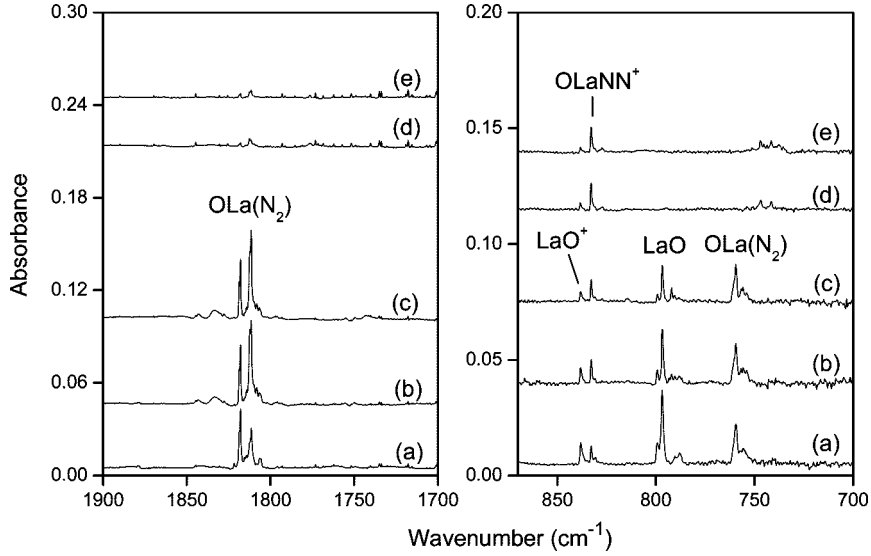

Figure 3. Infrared spectra in the 1900−1750 and 850−700 cm^{-1} regions from co-deposition of laser-ablated La atoms with 0.2% N_2O in Ar at 4 K. For the meaning of (a−e), see Figure 1.

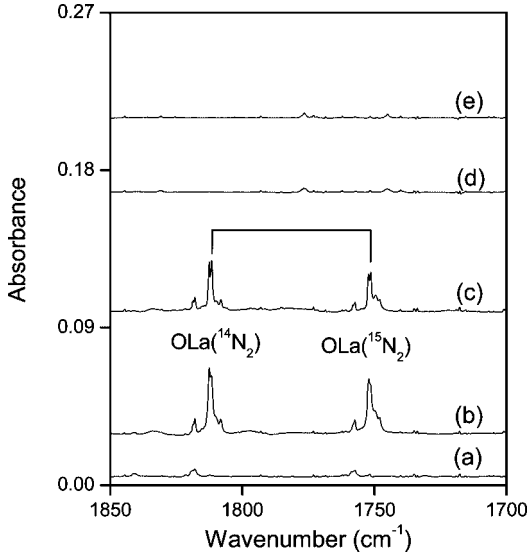

Figure 4. Infrared spectra in the 1850−1700 cm^{-1} region from co-deposition of laser-ablated La atoms with 0.15% $^{14}N_2O$ + 0.15% $^{15}N_2O$ in Ar at 4 K. For the meaning of (a−e), see Figure 1.

TABLE 1: IR Absorptions (in cm^{-1}) Observed from Co-deposition of Laser-Ablated Y and La Atoms with N_2O in Excess Argon at 4 K

$^{14}N_2O$	$^{15}N_2O$	$^{14}N_2O$ + $^{15}N_2O$	$^{14}N_2O/^{15}N_2O$	assignment
1839.4	1778.5	1839.4, 1778.5	1.0342	OYNN
1809.8	1749.7	1809.8, 1749.7	1.0343	$OY(N_2)$
866.2	866.2		1.0000	$OYNN^+$
802.3	802.3		1.0000	$OY(N_2)$
796.5	796.5		1.0000	OYNN
1817.9	1757.4	1817.9, 1757.4	1.0344	$OLa(N_2)$ site
1811.6	1751.4	1811.6, 1751.4	1.0344	$OLa(N_2)$
832.8	832.8		1.0000	$OLaNN^+$
759.4	759.4		1.0000	$OLa(N_2)$

bands. Furthermore, doping with CCl_4 has no effect on these bands (Figure 1, trace f), suggesting that these products are neutral.[29]

Our present DFT calculations show that the $OY(N_2)$ complex is the most stable isomer, followed by the OYNN complex, which is only 1.82 kcal/mol higher in energy than $OY(N_2)$ at the BP86 level (Figure 5). The Y-(η^2-NN)O and YNNO isomers

TABLE 2: Comparison of Observed and Calculated IR Frequencies (in cm^{-1}) and Isotopic Frequency Ratios for the Products

		observed		calculated		
species	vibrational mode	freq	$^{14}N_2O/^{15}N_2O$	method	freq	$^{14}N_2O/^{15}N_2O$
$OY(N_2)$	ν_{N-N}	1809.8	1.0343	BP86	1868.6	1.0349
				B3LYP	1927.9	1.0350
	ν_{Y-O}	802.3	1.0000	BP86	808.3	1.0000
				B3LYP	829.2	1.0000
OYNN	ν_{N-N}	1839.4	1.0342	BP86	1946.5	1.0350
				B3LYP	1980.5	1.0350
	ν_{Y-O}	796.5	1.0000	BP86	803.4	1.0000
				B3LYP	825.6	1.0000
$OYNN^+$	ν_{Y-O}	866.2	1.0000	BP86	885.3	1.0000
				B3LYP	909.2	1.0000
$OLa(N_2)$	ν_{N-N}	1811.6	1.0344	BP86	1880.0	1.0350
				B3LYP	1933.6	1.0350
	ν_{La-O}	759.4	1.0000	BP86	770.8	1.0000
				B3LYP	785.7	1.0000
$OLaNN^+$	ν_{La-O}	832.8	1.0000	BP86	866.2	1.0000
				B3LYP	884.3	1.0000

are about 66.9 and 78.4 kcal/mol higher in energy than $OY(N_2)$. The N−N stretching vibrational frequencies in the $OY(N_2)$, OYNN, Y-(η^2-NN)O, and YNNO complexes are predicted to be 1868.6, 1946.5, 1432.8, and 1358.0 cm^{-1} (Table 3), respectively. The features of the IR spectra in the present matrix experiments are reminiscent of those of the side-bonded structure of $OSc(N_2)$ and end-on-bonded structure of OScNN, in which the corresponding N−N stretching vibrational frequencies appear at 1817.2 and 1849.2 cm^{-1} in the argon matrix experiments, respectively.[15] Accordingly, the 1809.8 and 802.3 cm^{-1} bands are assigned to the N−N and Y−O stretching vibrations of the neutral $OY(N_2)$ complex and the 1839.4 and 796.5 cm^{-1} bands to the corresponding vibrations of the neutral OYNN complex on the basis of the results of the isotopic substitution, the N_2O concentration change, CCl_4-doping experiments, and the comparison with theoretical predictions.

The Y−O stretching vibrations in $OY(N_2)$ and OYNN are predicted to be 808.3 and 803.4 cm^{-1} (Table 3), which should be multiplied by 0.993 and 0.991 to fit the experimental values of 802.3 and 796.5 cm^{-1}, respectively, showing good scale factors.[32] As listed in Table 2, the calculated $^{14}N_2O/^{15}N_2O$

TABLE 3: Ground Electronic States, Point Groups, Vibrational Frequencies (in cm^{-1}), and Intensities (km/mol) of the Products Using the BP86 Functional

species	elec state	point group	frequency (intensity, mode)
$OY(N_2)$	$^2A''$	C_s	1868.6 (306, A′), 808.3 (181, A′), 322.9 (16, A′), 298.7 (16, A″), 160.8 (5, A″), 131.5 (21, A′)
OYNN	$^2A''$	C_s	1946.5 (689, A′), 803.4 (188, A′), 332.0 (4, A′), 239.3 (0.4, A″), 225.9 (36, A″), 106.3 (20, A′)
$OYNN^+$	$^1A'$	C_s	2341.9 (11, A′), 885.3 (118, A′), 220.7 (9, A″), 195.9 (12, A″), 177.7 (2, A″), 91.9 (28, A′)
$OLa(N_2)$	$^2A''$	C_s	1880.0 (425, A′), 770.8 (251, A′), 260.7 (12, A′), 260.5 (14, A″), 131.9 (5, A″), 105.3 (21, A′)
$OLaNN^+$	$^1A'$	C_s	2346.7 (17, A′), 866.2 (169, A′), 153.4 (1, A′), 136.9 (1, A″), 128.9 (11, A′), 20.3 (25, A′)

isotopic frequency ratios for the N−N and Y−O stretching vibrations are also in accord with experimental values. These agreements between the experimental and calculated vibrational frequencies, relative absorption intensities, and isotopic shifts confirm the identifications of the $OY(N_2)$ and OYNN complexes from the matrix IR spectra.

In the La + N_2O experiments, the N−N and La−O stretching vibrations for the analogous $OLa(N_2)$ complex have been observed at 1811.6 and 759.4 cm^{-1} (Table 1 and Figures 3 and 4), whereas those for the OLaNN complex are absent from the present experiments. The N−N and La−O stretching vibrations of the $OLa(N_2)$ complex are calculated to be 1880.0 and 770.8 cm^{-1} (Table 3), consistent with the experimental observations (1811.6 and 759.4 cm^{-1}, respectively) (Table 1).

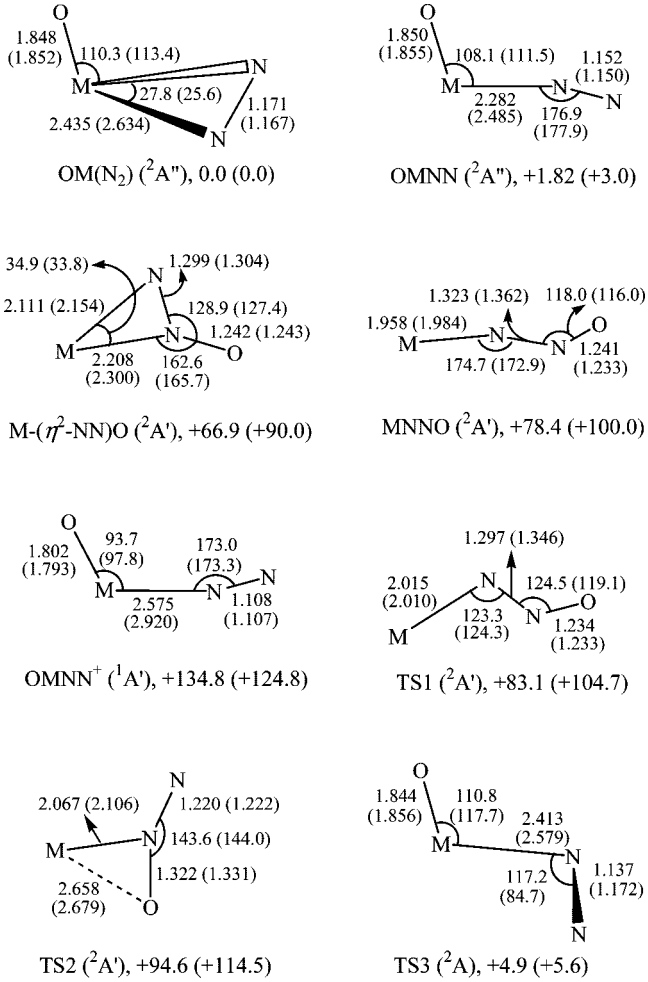

Figure 5. Optimized structures (bond lengths in angstroms, bond angles in degrees) and the relative energies (in kcal/mol) of the species involved in the reactions of N_2O with yttrium and lanthanum (in parentheses) atoms using the BP86 functional.

B. $OMNN^+$ (M = Y, La). In the Y + N_2O experiments, the absorption at 866.2 cm^{-1} that appears during sample deposition changes little after annealing and increases markedly upon broad-band irradiation at the expense of the neutral $OY(N_2)$ and OYNN complexes (Table 1 and Figure 1), indicating that this new product also has the YN_2O stiochiometry. The band at 866.2 cm^{-1}, which is in the spectral range expected for the terminal Y−O stretching mode,[31] shows no nitrogen isotopic shift. Doping with CCl_4 sharply increases this band (Figure 1, trace f), suggesting that the product is cationic.[29] By analogy with the $OScNN^+$ spectra,[15] the 866.2 cm^{-1} band is assigned to the Y−O stretching mode of the $OYNN^+$ cation. The corresponding IR absorption of the $OLaNN^+$ cation in solid argon has been observed at 832.8 cm^{-1} (Table 1 and Figure 3).

Our DFT calculations predict the $OYNN^+$ and $OLaNN^+$ complexes to have $^1A'$ ground states with C_s symmetry (Table 3 and Figure 5). For the $OYNN^+$ complex, the calculated Y−O stretching mode is 885.3 cm^{-1} (Table 3), which should be multiplied by 0.978 to fit the observed frequency, giving a reasonable scale factor.[32] The N−N stretching vibration is predicted to be 2341.9 cm^{-1}. With its small intensity (11 km/mol), it is not easy to be observed, consistent with the absence from the present experiments. Similar agreements have been obtained for the $OLaNN^+$ complex (Tables 1–3).

C. Reaction Mechanism and Bonding Consideration. On the basis of the behavior of sample annealing and irradiation, together with the observed species and calculated stable isomers, a plausible reaction mechanism can be proposed as follows. Under the present experimental conditions, the $OM(N_2)$ (M = Y, La) complexes are the primary products during sample deposition (Figures 1 and 3), suggesting that the spontaneous insertion of laser-ablated Y and La atoms into N_2O to form these side-bonded complexes is the dominant process (reactions 1–3). Taking the yttrium reaction as an example, the reaction starts by binding the outer nitrogen atom of N_2O with the yttrium atom to form a planar intermediate YNNO (reaction 1) (Figures 5 and 6). This step is predicted to be exothermic by 33.3 kcal/mol. Then, the isomerization proceeds by binding another nitrogen atom to form a side-bonded intermediate Y-(η^2-NN)O via transition state TS1. The barrier height for this process is predicted to be 4.7 kcal/mol. The oxygen atom can further be transferred to form the OYNN and/or $OY(N_2)$ products via transition states TS2 and TS3. It is noted that the barriers for these isomerizations are in the region of 2.7−27.8 kcal/mol (Figure 6), which can be obtained by radiation in the ablation plume. This finding is consistent with the gas-phase values (2−80 kcal/mol) in the previous kinetic studies on the reactions of N_2O with transition-metal atoms.[3–11] Figure 6 also reveals

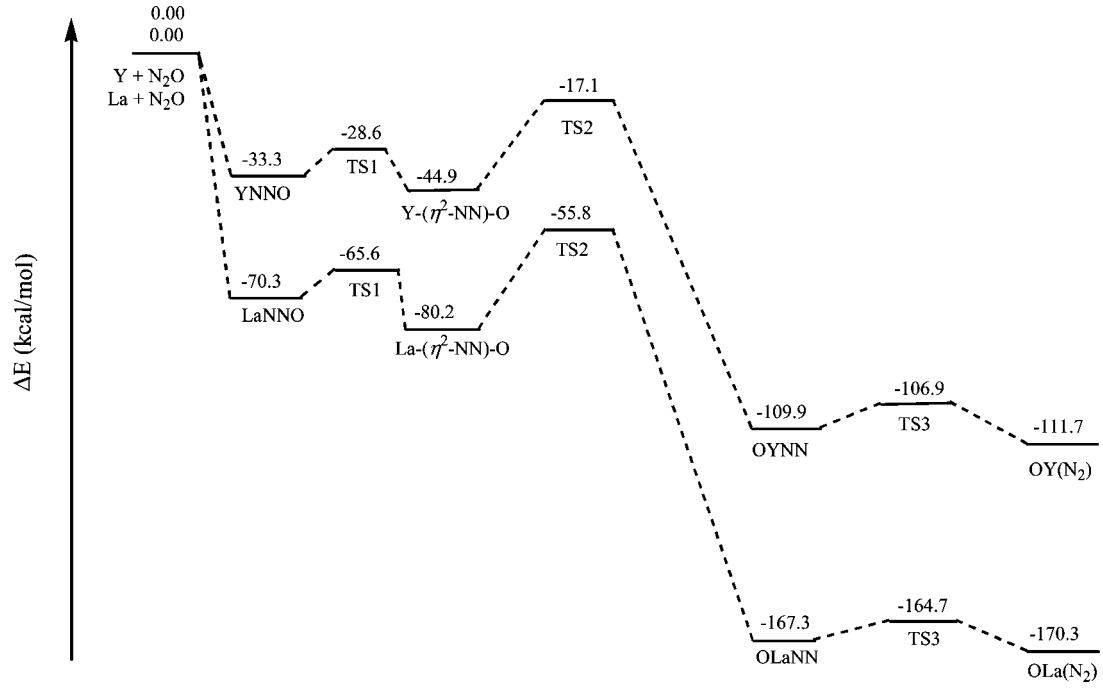

Figure 6. Potential energy surfaces of the reactions of N_2O with yttrium and lanthanum atoms using the BP86 functional.

that the isomerizations for lanthanum are more energetically favorable than those for yttrium. In contrast to the thermal evaporation technique, the laser ablation method produces more energetic atoms, allowing them to overpass energy barriers of some reactions;[29,33] the potential intermediate products (i.e. MNNO, M(η^2-NN)O, OLaNN) might be hopefully generated using the thermal evaporation technique.

$$M + N_2O \rightarrow MNNO \quad (M = Y, La) \tag{1}$$

$$MNNO \rightarrow M\text{-}(\eta^2\text{-}NN)O \tag{2}$$

$$M\text{-}(\eta^2\text{-}NN)O \rightarrow OMNN \text{ or } OM(N_2) \tag{3}$$

Recent investigations have shown that laser ablation of metal targets produces not only neutral metal atoms but also metal cations and electrons. Ionic metal complexes can also be formed in the reactions with small molecules.[29] In the present experiments, $OMNN^+$ cations appear during sample deposition and increase markedly upon broad-band irradiation at the expense of the neutral OMNN and $OM(N_2)$ complexes (Figures 1 and 3), suggesting that the $OMNN^+$ cations may be generated by photoionization of the neutral OMNN and $OM(N_2)$ complexes via radiation in the ablation plume and/or broad-band irradiation (reaction 4). The ionization energy of OMNN and $OM(N_2)$ is calculated to be about 130 kcal/mol, which exceeds the mercury arc energy (115 kcal/mol at 250 nm). This suggests that an OM(NN)* excited state is sufficiently long-lived to absorb a second photon to reach ionization. Furthermore, the NNO_2^- anion absorptions also increased upon broad-band irradiation, which serves as a counterion to preserve the matrix electric neutrality. Similar results have also been found for the Sc atom.[15]

$$OMNN \text{ or } OM(N_2) - e^- \rightarrow OMNN^+ \tag{4}$$

As illustrated in Figure 7, the highest occupied molecular orbitals (HOMOs) of $OM(N_2)$ and OMNN (M = Y, La) are π-type bonds, which comprise the synergic donations of filled orbitals of N_2 into an empty acceptor orbitals of MO and the back-donation of the MO electrons into the empty orbitals of N_2. Due to the different bonding modes, the primary donor

Figure 7. Molecular orbital depictions of the highest occupied molecular orbitals (HOMOs) of the $OM(N_2)$, OMNN, and $OMNN^+$ (M = Y, La) complexes.

orbitals in the side-bonded $OM(N_2)$ complexes are the filled $1\pi_u$ orbitals of N_2, whereas those in the end-on-bonded OMNN complexes are the filled $3\sigma_g$ orbitals of N_2. The single-occupied δ orbitals are the back-donation orbitals. These bonding features are similar to those of the OScNN and $OSc(N_2)$ complexes.[15] For the $OMNN^+$ complexes, there is no obvious orbital overlap between the MO and N_2 fragments, as shown in Figure 7, and the bonding interaction is mainly electrostatic between the MO^+ cations and the N_2 fragment.

Conclusions

Reactions of laser-ablated yttrium and lanthanum atoms with nitrous oxide molecules in excess argon have been investigated using matrix-isolation infrared spectroscopy. In the Y + N_2O experiments, the absorptions at 1809.8 and 802.3 cm^{-1} are assigned to the N−N and Y−O stretching vibrations of the neutral $OY(N_2)$ complex, and the absorptions at 1839.4 and 796.5 cm^{-1} are assigned to the corresponding vibrations of the neutral OYNN complex on the basis of the results of the isotopic substitution, the N_2O concentration change, CCl_4-doping experiments, and the comparison with theoretical predictions. An analogous $OLa(N_2)$ complex has also been obtained in the La reaction. IR spectroscopy also provides evidence for the formation of the $OYNN^+$ and $OLaNN^+$ cation complexes. Bonding analysis reveals that the highest occupied molecular orbitals of $OM(N_2)$ and OMNN (M = Y, La) are π-type bonds, which comprise the synergic donations of filled orbitals of N_2 into empty orbitals of MO and the back-donation of the MO electrons into the empty orbitals of N_2. The bonding interaction

in the $OMNN^+$ complexes is mainly electrostatic between the MO^+ cations and the N_2 fragment.

Acknowledgment. The authors would like to express thanks to the reviewers for valuable suggestions. This work was supported by AIST and a Grant-in-Aid for Scientific Research (B) (Grant No. 17350012) from the Ministry of Education, Culture, Sports, Science and Technology (MEXT) of Japan. L.J. is grateful to the Japan Society for Promotion of Science (JSPS) for a postdoctoral fellowship.

References and Notes

(1) Trogler, W. C. *Coord. Chem. Rev.* **1999**, *187*, 303.

(2) (a) Kapteijn, F.; Rodriguez-Mirasol, J.; Moulijn, J. A. *Appl. Catal. B* **1996**, *9*, 25. (b) Dandekar, A.; Vannice, M. A. *Appl. Catal. B* **1999**, *22*, 179. (c) Burch, R.; Daniells, S. T.; Breen, J. P.; Hu, P. *J. Catal.* **2004**, *224*, 252.

(3) Armentrout, P. B.; Halle, L. F.; Beauchamp, J. L. *J. Chem. Phys.* **1982**, *76*, 2449.

(4) Ritter, D.; Weisshaar, J. C. *J. Phys. Chem.* **1989**, *93*, 1576.

(5) Ritter, D.; Weisshaar, J. C. *J. Phys. Chem.* **1990**, *94*, 4907.

(6) Futerko, P. M.; Fontijn, A. *J. Chem. Phys.* **1991**, *95*, 8065, and references therein.

(7) Futerko, P. M.; Fontijn, A. *J. Chem. Phys.* **1992**, *97*, 3861.

(8) Futerko, P. M.; Fontijn, A. *J. Chem. Phys.* **1993**, *98*, 7004.

(9) Campbell, M. L. *J. Chem. Soc., Faraday Trans.* **1998**, *94*, 1687, and references therein.

(10) (a) Stirling, A. *J. Phys. Chem. A* **1998**, *102*, 6565. (b) Stirling, A. *J. Am. Chem. Soc.* **2002**, *124*, 4058.

(11) Campbell, M. L.; Kolsch, E. J.; Hooper, K. L. *J. Phys. Chem. A* **2000**, *104*, 11147.

(12) Herschbach, D. R. *Adv. Chem. Phys.* **1996**, *10*, 319.

(13) (a) For example, see: Xu, C.; Manceron, L.; Perchard, J. P. *J. Chem. Soc., Faraday Trans.* **1993**, *89*, 1291. (b) Bondybey, V. E.; Smith, A. M.; Agreiter, J. *Chem. Rev.* **1996**, *96*, 2113. (c) Fedrigo, S.; Haslett, T. L.; Moskovits, M. *J. Am. Chem. Soc.* **1996**, *118*, 5083. (d) Khriachtchev, L.; Pettersson, M.; Runeberg, N.; Lundell, J.; Rasanen, M. *Nature* **2000**, *406*, 874. (e) Himmel, H. J.; Manceron, L.; Downs, A. J.; Pullumbi, P. *J. Am. Chem. Soc.* **2002**, *124*, 4448. (f) Li, J.; Bursten, B. E.; Liang, B.; Andrews, L. *Science* **2002**, *295*, 2242. (g) Andrews, L.; Wang, X. *Science* **2003**, *299*, 2049.

(14) (a) Zhou, M. F.; Tsumori, N.; Li, Z.; Fan, K.; Andrews, L.; Xu, Q. *J. Am. Chem. Soc.* **2002**, *124*, 12936. (b) Zhou, M. F.; Xu, Q.; Wang, Z.; Schleyer, P. v. R. *J. Am. Chem. Soc.* **2002**, *124*, 14854. (c) Jiang, L.; Xu, Q. *J. Am. Chem. Soc.* **2005**, *127*, 42. (d) Xu, Q.; Jiang, L.; Tsumori, N. *Angew. Chem., Int. Ed.* **2005**, *44*, 4338. (e) Jiang, L.; Xu, Q. *J. Am. Chem. Soc* **2005**, *127*, 8906. (f) Jiang, L.; Xu, Q. *J. Am. Chem. Soc.* **2006**, *128*, 1394, Addition and Correction.

(15) Zhou, M. F.; Wang, G. J.; Zhao, Y. Y.; Chen, M. H.; Ding, C. F. *J. Phys. Chem. A* **2005**, *109*, 5079.

(16) Chertihin, G. V.; Andrews, L. *J. Phys. Chem.* **1994**, *98*, 5891.

(17) Jin, X.; Wang, G. J.; Zhou, M. F. *J. Phys. Chem. A* **2006**, *110*, 8017.

(18) Wang, G. J.; Zhou, M. F. *Chem. Phys.* **2007**, *342*, 90.

(19) Wang, G. J.; Jin, X.; Chen, M. H.; Zhou, M. F. *Chem. Phys. Lett.* **2006**, *420*, 130.

(20) (a) Burkholder, T. R.; Andrews, L. *J. Chem. Phys.* **1991**, *95*, 8697. (b) Zhou, M. F.; Tsumori, N.; Andrews, L.; Xu, Q. *J. Phys. Chem. A* **2003**, *107*, 2458. (c) Jiang, L.; Xu, Q. *J. Chem. Phys.* **2005**, *122*, 034505. (d) Jiang, L.; Teng, Y. L.; Xu, Q. *J. Phys. Chem. A* **2006**, *110*, 7092.

(21) Frisch, M. J. Trucks, G. W.; Schlegel, H. B.; Scuseria, G. E.; Robb, M. A.; Cheeseman, J. R.; Montgomery, J. A., Jr.; Vreven, T.; Kudin, K. N.; Burant, J. C.; Millam, J. M.; Iyengar, S. S.; Tomasi, J.; Barone, V.; Mennucci, B.; Cossi, M.; Scalmani, G.; Rega, N.; Petersson, G. A.; Nakatsuji, H.; Hada, M.; Ehara, M.; Toyota, K.; Fukuda, R.; Hasegawa, J.; Ishida, M.; Nakajima, T.; Honda, Y.; Kitao, O.; Nakai, H.; Klene, M.; Li, X.; Knox, J. E.; Hratchian, H. P.; Cross, J. B.; Bakken, V.; Adamo, C.; Jaramillo, J.; Gomperts, R.; Stratmann, R. E.; Yazyev, O.; Austin, A. J.; Cammi, R.; Pomelli, C.; Ochterski, J. W.; Ayala, P. Y.; Morokuma, K.; Voth, G. A.; Salvador, P.; Dannenberg, J. J.; Zakrzewski, V. G.; Dapprich, S.; Daniels, A. D.; Strain, M. C.; Farkas, O.; Malick, D. K.; Rabuck, A. D.; Raghavachari, K.; Foresman, J. B.; Ortiz, J. V.; Cui, Q.; Baboul, A. G.; Clifford, S.; Cioslowski, J.; Stefanov, B. B.; Liu, G.; Liashenko, A.; Piskorz, P.; Komaromi, I.; Martin, R. L.; Fox, D. J.; Keith, T.; Al-Laham, M. A.; Peng, C. Y.; Nanayakkara, A.; Challacombe, M.; Gill, P. M. W.; Johnson, B.; Chen, W.; Wong, M. W.; Gonzalez, C.; Pople, J. A. *Gaussian 03*, revision B.04; Gaussian, Inc.: Pittsburgh, PA, 2003.

(22) (a) Becke, A. D. *Phys. Rev. A* **1988**, *38*, 3098. (b) Perdew, J. P. *Phys. Rev. B* **1986**, *33*, 8822. (c) Lee, C.; Yang, E.; Parr, R. G. *Phys. Rev. B* **1988**, *37*, 785. (d) Becke, A. D. *J. Chem. Phys.* **1993**, *98*, 5648.

(23) (a) McLean, A. D.; Chandler, G. S. *J. Chem. Phys.* **1980**, *72*, 5639. (b) Krishnan, R.; Binkley, J. S.; Seeger, R.; Pople, J. A. *J. Chem. Phys.* **1980**, *72*, 650.

(24) Andrae, D.; Haeussermann, U.; Dolg, M.; Stoll, H.; Preuss, H. *Theor. Chim. Acta* **1990**, *77*, 123.

(25) Ayala, P. Y.; Schlegel, H. B. *J. Chem. Phys.* **1997**, *107*, 375.

(26) (a) Peng, C.; Schlegel, H. B. *Isr. J. Chem.* **1994**, *33*, 449. (b) Peng, C.; Ayala, P. Y.; Schlegel, H. B.; Frisch, M. J. *J. Comput. Chem.* **1996**, *17*, 49.

(27) (a) Gonzalez, C.; Schlegel, H. B. *J. Chem. Phys.* **1989**, *90*, 2154. (b) Gonzalez, C.; Schlegel, H. B. *J. Phys. Chem.* **1990**, *94*, 5523.

(28) (a) Gutsev, G. L.; Andrews, L.; Bauschlicher, C. W., Jr. *Theor. Chem. Acc.* **2003**, *109*, 298. (b) Jiang, L.; Xu, Q. *J. Chem. Phys.* **2008**, *128*, 124317.

(29) Zhou, M. F.; Andrews, L.; Bauschlicher, C. W., Jr. *Chem. Rev.* **2001**, *101*, 1931, and references therein.

(30) Darling, J. H.; Ogden, J. S. *J. Chem. Soc., Dalton Trans.* **1972**, 2496.

(31) Andrews, L.; Zhou, M. F.; Chertihin, G. V.; Bauschlicher, C. W., Jr. *J. Phys. Chem. A* **1999**, *103*, 6525.

(32) Merrick, J. P.; Moran, D.; Radom, L. *J. Phys. Chem. A* **2007**, *111*, 11683.

(33) Himmel, H. J.; Downs, A. J.; Greene, T. M. *Chem. Rev.* **2002**, *102*, 4191, and references therein.

JP802114Z